Dalton Transactions

PAPER

View Article Online
View Journal | View Issue



Cite this: *Dalton Trans.*, 2015, **44**, 19282

# Pentanuclear [2.2] spirocyclic lanthanide(III) complexes: slow magnetic relaxation of the $Dy^{III}$ analogue†

Sourav Biswas,[a] Sourav Das,[a,b] Jan van Leusen,[c] Paul Kögerler*[c] and Vadapalli Chandrasekhar*[a,d]

Received 8th August 2015,
Accepted 4th October 2015

DOI: 10.1039/c5dt03060a

www.rsc.org/dalton

The reaction of $LnCl_3{\cdot}6H_2O$ (Ln = $Dy^{3+}$, $Tb^{3+}$ and $Ho^{3+}$) with the multisite coordinating ligand *N*′-(2-hydroxy-3-(hydroxymethyl)-5-methylbenzylidene)acetohydrazide ($LH_3$) in the presence of pivalic acid (PivH) leads to the formation of three isostructural homometallic pentanuclear complexes, $[Dy_5(LH)_4(\eta^1\text{-Piv})(\eta^2\text{-Piv})_3(\mu_2\text{–}\eta^2\eta^1\text{Piv})_2(H_2O)]{\cdot}Cl{\cdot}9{\cdot}5H_2O{\cdot}5MeOH$ (**1**), $[Tb_5(LH)_4(\eta^1\text{-Piv})(\eta^2\text{-Piv})_3(\mu_2\text{–}\eta^2\eta^1\text{-Piv})_2(H_2O)]{\cdot}Cl{\cdot}10.5H_2O{\cdot}2MeOH{\cdot}2CHCl_3$ (**2**) and $[Ho_5(LH)_4(\eta^1\text{-Piv})(\eta^2\text{-Piv})_3(\mu_2\text{–}\eta^2\eta^1\text{Piv})_2(H_2O)]{\cdot}Cl{\cdot}14.5\text{-}H_2O{\cdot}2CHCl_3$ (**3**). **1–3** are monocationic and are comprised of four doubly deprotonated $[LH]^{2-}$ ligands along with six pivalate ions. These complexes possess a [2.2] spirocyclic topology formed by the fusion of two triangles of $Ln^{III}$ ions at a common vertex. The magneto chemical analysis reveals the presence of antiferromagnetic exchange interactions at low temperature, and the $Dy^{III}$ complex **1** gives an out-of-phase signal with a small curvature in alternating current (ac) magnetic susceptibility measurement. Application of a 3000 G static field during ac measurement intensifies the signals, revealing a second slow relaxation process in the $Dy^{III}$ analogue.

## Introduction

The synthesis of polynuclear clusters of 4f metal ions is of interest because of their potential utility in single-molecule magnets (SMMs), catalysis,[1] luminescence,[2] medical imaging,[3] magnetic refrigeration,[4] high-density data storage,[5] spintronics[6] and quantum computing.[7] SMMs are characterized by a slow relaxation of magnetization below the blocking temperature, $T_B$. Magnetic phenomena have been thoroughly explored in polynuclear 3d metal complexes[8,9] and heterometallic 3d/4f complexes,[10] and the recent years have seen the emergence of lanthanide complexes, particularly those involving $Dy^{3+}$ or $Tb^{3+}$. Here, the zero-field splitting of the $m_J$ sub-states belonging to the *J* ground state produces the thermal energy barriers. Interest in lanthanide complex SMMs has been fueled by the seminal discovery by Winpenny and co-workers of complexes $[Dy_4K_2O(O^tBu)_{12}]$ and $[Dy_5O(O^iPr)_{13}]$, possessing exceptionally high energy barriers for magnetization reversal.[11] Homometallic 4f complexes of varying nuclearities (Ln,[12] $Ln_2$,[13] $Ln_3$,[14] $Ln_4$,[15] $Ln_5$,[16] $Ln_6$,[17] $Ln_7$,[18] $Ln_8$,[19] $Ln_9$,[20] $Ln_{10}$ [21] and $Ln_{11}$ [22]) are now documented in the literature, and we have reported new SMMs involving 3d/4f[23] and 4f[24] metal ions. The five examples of pentanuclear lanthanide complexes known display three distinct structural topologies: pyramidal,[16a–c] butterfly[16e] and trigonal bipyramidal.[16d] These pentanuclear complexes evince SMM behavior including Winpenny's $[Dy_5O(O^iPr)_{13}]$ complex, which showed a slow relaxation of magnetization with a 528 ± 11 K thermal energy barrier.[16a] To pursue new polynuclear lanthanide complexes, we have designed a new linear alkyl hydrazone-based multidentate Schiff base ligand, *N*′-(2-hydroxy-3-(hydroxymethyl)-5-methylbenzylidene)acetohydrazide ($LH_3$); upon reaction with $LnCl_3{\cdot}6H_2O$ (Ln = $Dy^{3+}$, $Tb^{3+}$ and $Ho^{3+}$), this afforded homometallic pentanuclear [2.2] spirocyclic complexes **1–3**, $[Ln_5(LH)_4(\eta^1\text{-Piv})(\eta^2\text{-Piv})_3(\mu_2\text{–}\eta^2\eta^1\text{Piv})_2(H_2O)]{\cdot}Cl{\cdot}xH_2O{\cdot}y\text{MeOH}{\cdot}z\text{CHCl}_3$ ($Dy^{3+}$, $x$ = 9.5, $y$ = 5, $z$ = 0; $Tb^{3+}$, $x$ = 10.5, $y$ = 2, $z$ = 2 and $Ho^{3+}$, $x$ = 14.5, $y$ = 0, $z$ = 2).

[a]*Department of Chemistry, Indian Institute of Technology Kanpur, Kanpur-208016, India. E-mail: vc@iitk.ac.in, paul.koegerler@ac.rwth-aachen.de; http://www.iitk.ac.in*
[b]*Department of Emerging Materials Science, DGIST, Daegu 711-873, Korea*
[c]*Institut für Anorganische Chemie, RWTH Aachen University, D-52074 Aachen, Germany. http://www.ac.rwth-aachen.de*
[d]*National Institute of Science Education and Research, Institute of Physics Campus, Sachivalaya Marg, PO: Sainik School, Bhubaneswar-751 005, India. http://www.niser.ac.in*

†Electronic supplementary information (ESI) available. Molecular structures of **2** and **3** (Fig. S1–S2), list of bond lengths and bond angles (Tables S1–S2), Cole–Cole plot at zero dc field (Fig. S3), $\chi'_m$ *vs.* *T* plot at 3000 G (Fig. S4), $\chi''_m$ *vs.* *T* at 3000 G (Fig. S5), $\tau$ *vs.* $T^{-1}$ (Fig. S6), PXRD (Fig. S6–S8), reported Ln5 complexes (Fig. S9) and TGA (Fig. S10–S12). CCDC 1031235–1031237. For ESI and crystallographic data in CIF or other electronic format see DOI: 10.1039/c5dt03060a

In these complexes two triangles of $Ln^{3+}$ ions are fused through a common vertex. The synthesis, structure and magnetic properties of these complexes are discussed herein.

## Results and discussion

### Synthesis

Ligand design is a crucial element in modulating the nuclearity and structural topology of lanthanide complexes. Recently, we have prepared rhombus-shaped $Ln_4$ complexes, $[Ln_4(LH)_2(\mu_2\text{-}O)_4(H_2O)_8]$ (Ln = $Dy^{3+}$ and $Ho^{3+}$),[25] incorporating an aroyl hydrazone-based Schiff base ligand (6-hydroxymethyl)-*N*′-((8-hydroxyquinolin-2-yl)-methylene)picolinohydrazide (Scheme 1a).

Motivated by this work, as well as by the use of other hydrazone-based Schiff base ligands in the recent literature,[14c,15d,17d,24,26] we have prepared a multisite coordinating semi-flexible alkyl hydrazone-based ligand, *N*′-(2-hydroxy-3-(hydroxymethyl)-5-methylbenzylidene)acetohydrazide ($LH_3$). This was produced using a two-step synthetic protocol that involved the preparation of B1, which subsequently undergoes a condensation reaction with B2 to give $LH_3$ (Scheme 2). The semi flexible ligand, $LH_3$ provides five divergent coordinating sites: an alkyl hydrazone oxygen, an imine N, an amide N, a phenolic O and a flexible $-CH_2OH$ arm. The latter is a crucial element in the formation of the coordination geometry, as recently shown by us in the preparation of cubane-shaped tetranuclear lanthanide complexes (Scheme 1b).[27] The pivalic acid co-ligands help to saturate the primary coordination spheres of the metals by bridging the metal centers, and confers lipophilicity to the complexes.

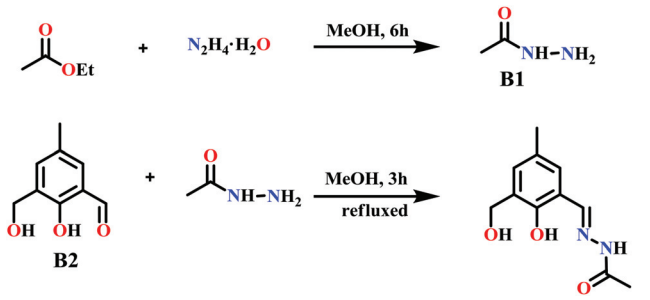


Scheme 2 Synthesis of the ligand $LH_3$.

The reaction of $LH_3$, $LnCl_3{\cdot}6H_2O$, and pivalic acid in the stoichiometric ratio of 4 : 5 : 6 in the presence of 4 equivalents of triethylamine in methanol afforded pentanuclear complexes $[Ln_5(LH)_4(\eta^1\text{-Piv})(\eta^2\text{-Piv})_3(\mu_2\text{–}\eta^2\ \ \eta^1\text{Piv})_2(H_2O)]{\cdot}Cl{\cdot}xH_2O{\cdot}yMeOH{\cdot}zCHCl_3$ [compound **1**, Ln = $Dy^{3+}$, $x$ = 9.5, $y$ = 5, $z$ = 0; compound **2**, Ln = $Tb^{3+}$, $x$ = 10.5, $y$ = 2, $z$ = 2 and compound **3**, Ln = $Ho^{3+}$, $x$ = 14.5, $y$ = 0, $z$ = 2] (Scheme 3).

### X-ray crystal structures

Single-crystal X-ray diffraction measurements reveal that compounds **1–3** are isostructural, and crystallize in the tetragonal

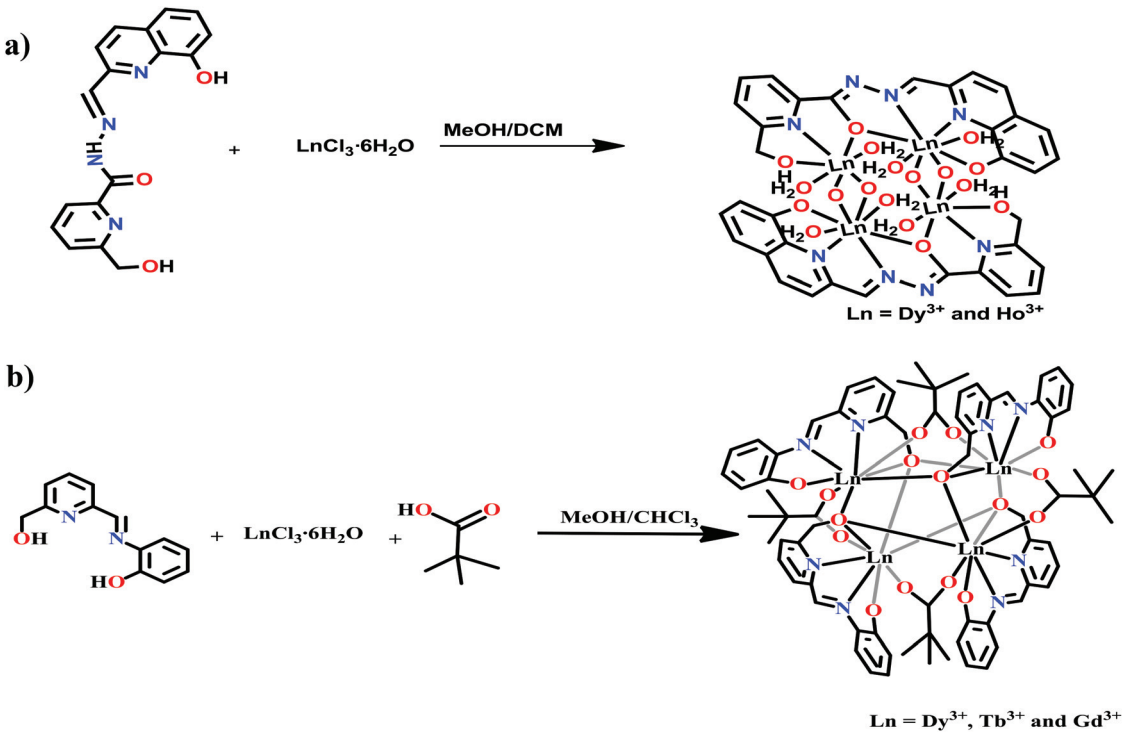


Scheme 1 (a) Synthesis of rhombus-shaped tetranuclear lanthanide complexes[25] (b) Synthesis of cubane-shaped tetranuclear lanthanide complexes.[27]

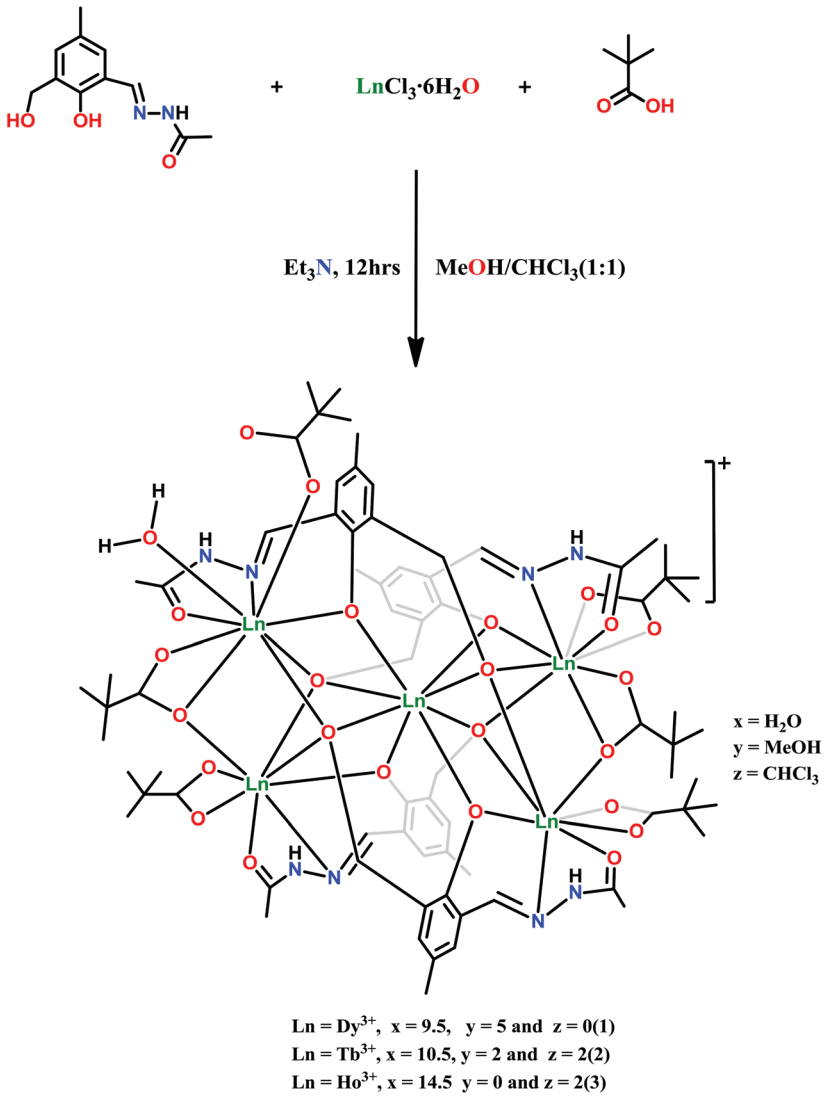


**Scheme 3** Synthesis of $[Ln_5(LH)_4(\eta^1\text{-Piv})(\eta^2\text{-Piv})_3(\mu_2\text{–}\eta^2\ \eta^1\text{Piv})_2(H_2O)]\cdot Cl\cdot xH_2O\cdot y\text{MeOH}\cdot z\text{CHCl}_3$ (Dy, $x$ = 9.5, $y$ = 5, $z$ = 0; Tb, $x$ = 10.5, $y$ = 2, $z$ = 2 and Ho, $x$ = 14.5, $y$ = 0, $z$ = 2).

space group $I\bar{4}$ with $Z$ = 4. The complexes are monocationic, with their charges each balanced by a chloride anion, and possess a [2.2] spirocycle of $Ln^{III}$ ions containing two fused triangular motifs. Complex **1** has been chosen as a representative example to illustrate the common structural features of these clusters. Selected bond parameters of **1** are summarized in Table 1. The molecular structure and selected bond parameters of the other complexes (**2** and **3**) are presented in the ESI (Fig. S1–S2† and Tables S1–S2†). A perspective view of the molecular structure of **1** is depicted in Fig. 1.

The pentanuclear complex **1** is formed by the concerted coordination action of the four doubly deprotonated ligands $[LH]^{2-}$. Four out of five potential coordinating sites of the ligand are coordinated to the metal centers: a phenolate oxygen which functions as a bridging ligand between two $Dy^{3+}$ centers, a deprotonated hydroxymethyl arm which functions as a $\mu_3$-capping ligand among three $Dy^{III}$ centers, an imine nitrogen binding a $Dy^{3+}$ center, and an acetohydrazide oxygen coordinating a $Dy^{3+}$ center. The framework provided by the ligand $[LH]^{2-}$ is bolstered by the coordination of six pivalate ligands: one is $\eta^1$-coordinated to Dy4, while three others chelate Dy1, Dy2 and Dy5 in an $\eta^2$ fashion. The remaining two pivalate ligands exhibit both bridging and chelating modes ($\mu_2$–$\eta^2$:$\eta^1$) in their coordination that links Dy1 to Dy2 and Dy4 to Dy5. The pentanuclear [2.2] spirocyclic core is thus constructed by the coordination action of four $[LH]^{2-}$ ($\mu_4$–$\eta^3$:$\eta^2$:$\eta^1$:$\eta^1$) and six pivalate ligands. The coordination modes of the ligands are depicted in Fig. 2.

The pentacationic pentanuclear core, $[Dy_5(\mu_3\text{-O})_4(\mu_2\text{-O})_4(\mu_2\text{–}\eta^2\eta^1\text{Piv})_2]^{5+}$ consists of two $Dy_3$ triangles which are interconnected by sharing a common vertex, Dy3. The remaining four vertices of the two triangles are occupied by Dy1, Dy2, Dy4 and Dy5 (Fig. 3a). The edges of the triangles are formed by the pivalate ligands as well as phenolate oxygens of the ligand

 

Table 1 Selected bond distances (Å) and bond angles (°) parameters for **1**

| | | | | | |
|---|---|---|---|---|---|
| **Selected bond length around Dy1** | | Dy(3)–O(11) | 2.351(6) | Dy(5)–O(10) | 2.409(6) |
| Dy(1)–O(11) | 2.310(6) | Dy(3)–O(4) | 2.351(6) | Dy(5)–O(18) | 2.456(9) |
| Dy(1)–O(12) | 2.396(7) | Dy(3)–O(4) | 2.351(6) | Dy(5)–N(7) | 2.508(9) |
| Dy(1)–O(20) | 2.409(7) | Dy(3)–O(1) | 2.353(6) | | |
| Dy(1)–O(9) | 2.417(6) | Dy(3)–O(2) | 2.381(7) | **Selected Bond angles around Dy** | |
| Dy(1)–O(19) | 2.442(7) | Dy(3)–O(5) | 2.414(6) | Dy(2)–O(1)–Dy(1) | 97.9(2) |
| Dy(1)–O(21) | 2.447(6) | | | Dy(3)–O(1)–Dy(1) | 94.3(2) |
| Dy(1)–O(1) | 2.457(6) | **Selected bond length around Dy4** | | Dy(5)–O(2)–Dy(3) | 97.2(2) |
| Dy(1)–N(1) | 2.519(8) | Dy(4)–O(15) | 2.312(7) | Dy(3)–O(4)–Dy(5) | 95.2(2) |
| Dy(1)–O(22) | 2.521(6) | Dy(4)–O(8) | 2.373(6) | Dy(3)–O(4)–Dy(4) | 96.9(2) |
| | | Dy(4)–O(7) | 2.384(7) | Dy(5)–O(4)–Dy(4) | 99.5(2) |
| **Selected bond length around Dy2** | | Dy(4)–O(4) | 2.396(6) | Dy(2)–O(5)–Dy(3) | 95.3(2) |
| Dy(2)–O(24) | 2.320(7) | Dy(4)–O(30) | 2.411(7) | Dy(3)–O(8)–Dy(4) | 98.4(2) |
| Dy(2)–O(5) | 2.324(6) | Dy(4)–N(4) | 2.494(8) | Dy(3)–O(9)–Dy(1) | 95.9(2) |
| Dy(2)–O(22) | 2.325(6) | Dy(4)–O(10) | 2.500(6) | Dy(3)–O(9)–Dy(2) | 94.5(2) |
| Dy(2)–O(1) | 2.333(6) | Dy(4)–O(14) | 2.505(8) | Dy(1)–O(9)–Dy(2) | 96.18(9) |
| Dy(2)–O(6) | 2.402(7) | Dy(4)–O(13) | 2.666(9) | Dy(3)–O(10)–Dy(5) | 96.0(2) |
| Dy(2)–O(9) | 2.439(6) | | | Dy(3)–O(10)–Dy(4) | 95.4(2) |
| Dy(2)–N(5) | 2.450(8) | **Selected bond length around Dy5** | | Dy(5)–O(10)–Dy(4) | 96.1(2) |
| Dy(2)–O(23) | 2.454(7) | Dy(5)–O(13) | 2.258(7) | Dy(1)–O(11)–Dy(3) | 98.3(2) |
| | | Dy(5)–O(2) | 2.286(6) | Dy(5)–O(13)–Dy(4) | 95.4(3) |
| **Selected bond length around Dy3** | | Dy(5)–O(17) | 2.356(11) | Dy(2)–O(22)–Dy(1) | 96.4(2) |
| Dy(3)–O(10) | 2.301(6) | Dy(5)–O(3) | 2.381(7) | Dy(2)–O(1)–Dy(3) | 96.7(2) |
| Dy(3)–O(8) | 2.321(6) | Dy(5)–O(4) | 2.387(6) | | |
| Dy(3)–O(9) | 2.330(6) | | | | |

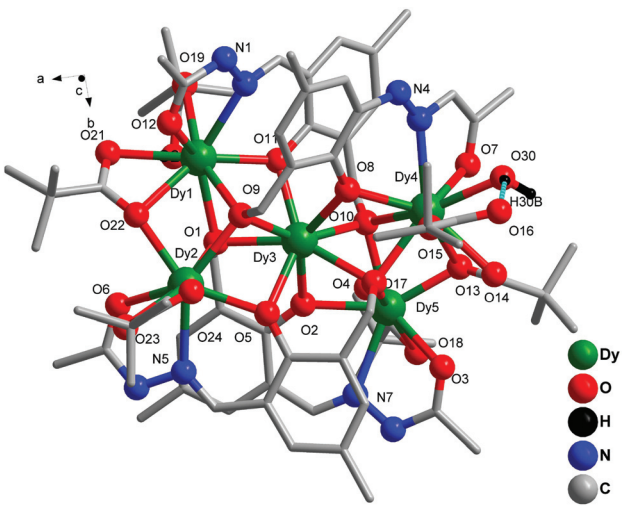


Fig. 1 Molecular structure of **1** (selected hydrogen atoms, chloride and the solvent molecules have been omitted for clarity).

$[LH]^{2-}$ while the faces of the triangle are effectively capped by $\mu_3$-O, emanating from the flexible pendant hydroxymethyl arms (Fig. 3a). The capping $\mu_3$ oxygen atoms lie at an average of ~1.219 Å away from the two triangular planes. The triangles are nearly equilateral, with Dy···Dy vertex lengths of 3.50–3.651 Å and Dy–Dy–Dy angles that range from 58.1°–62.2°. The two triangles are twisted at the Dy3 [2.2] spirocyclic node by a dihedral angle 55.85° (Fig. 3b).

The five crystallographically independent lanthanide centers present in **1** can be classified into three coordination geometry types (all distorted): triangular dodecahedron (Dy1, Dy5), square antiprism (Dy3), and mono-capped square-anti-prism (Dy2, Dy4) (Fig. 4). A minor variation exists in the coordination environment around Dy2 and Dy4: unlike the rest of the dysprosium centers, Dy4 is coordinated by a water molecule, which is engaged in strong hydrogen bonding with the oxygen atom of the $\eta^1$-pivalate ligand (Fig. 1) (D–H···A distance 1.746 Å and angle 154.41°) accounting for the $\eta^1$ binding mode rather than the anticipated $\eta^2$ coordination mode of the

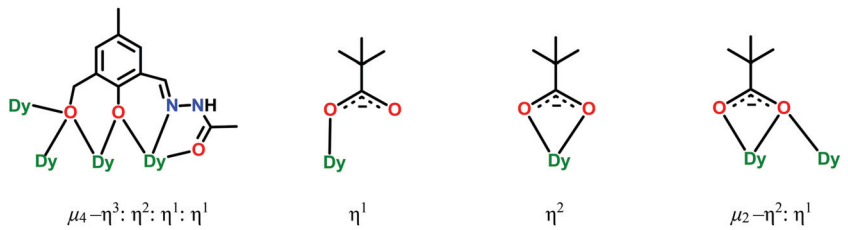


Fig. 2 Binding modes of $[LH]^{2-}$ and the pivalate ligands with $Dy^{3+}$ ions in **1**.

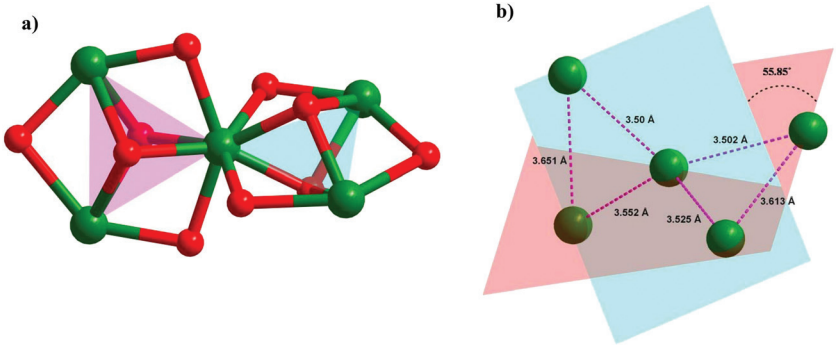


Fig. 3 (a) [2.2] spirocyclic core of the complex **1** (b). [2.2] spirocyclic core showing the dihedral angle between the two triangular motifs along with the distance between the $Dy^{3+}$ centers.

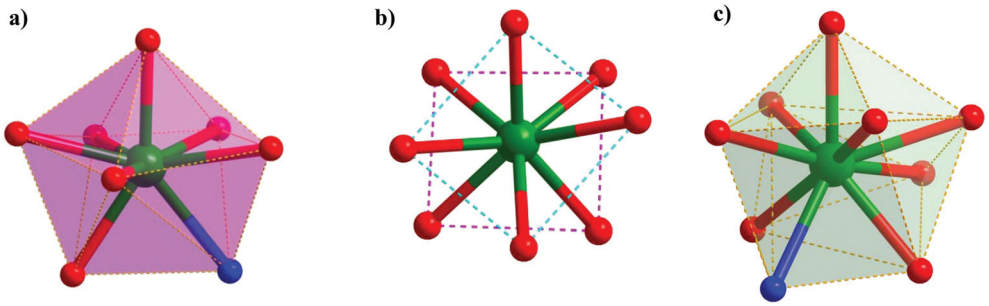


Fig. 4 Local geometry around the three types of dysprosium centres in **1**: (a) Dy1 and Dy5 possessing a distorted triangular dodecahedral geometry, (b) Dy3 possessing a distorted square antiprism geometry and (c) Dy2 and Dy4 possessing a distorted monocapped square antiprism.

pivalate ligand. The $Dy–O_{phenoxy}$ bond lengths fall in the range of ~2.286–2.414 Å which are slightly shorter than the $Dy–O_{alkoxy}$ bond lengths (~2.330–2.457 Å). These are in turn shorter than many $Dy–O_{piv}$ bond distances that range from ~2.258 to ~2.660 Å. Bond lengths involving the coordinated imine nitrogens lie in the range of ~2.449–2.519 Å. The $Dy–O_{phen}–Dy$ (95.31°–98.36°) and $Dy–O_{piv}–Dy$ angles (95.36–96.36°) are in a similar range.

The [2.2] spirocyclic topology observed in complexes **1–3** is quite distinct from the pyramidal,[16a–c] butterfly[16e] or trigonal bipyramidal[16d] shaped homometallic $Ln_5$ clusters reported previously (Fig. S9†). A comparison of the geometry around the metal centers, the structural topology around the metal ions and the SMM properties of the pentanuclear lanthanide families are summarized in Table 2.

### Thermogravimetric study of complex 1–3

Thermogravimetric analysis reveals that all the complexes **1–3** exhibit almost a similar decomposition pattern towards heat treatment involving a two-step weight loss process (Fig. S10–S12†). A small weight loss in the region of 60–120 °C was observed for all the complexes which is in part due to the loss of solvents of crystallization. In all the cases, some of the solvent molecules of crystallization are lost rapidly as the crystals are brought outside the mother liquor at room temperature. In the second step, above 300 °C, rapid weight loss of all the complexes was observed, confirming the decomposition of the complexes.

### Magnetic studies

Direct current (dc) magnetic susceptibility data for **1–3** are presented as $\chi_m T$ *vs.* $T$ curves at $B = 0.1$ Tesla, and molar magnetization $M_m$ *vs.* applied field $B$ diagrams at $T = 2$ K in Fig. 5. For the $Dy^{III}$ analogue **1**, $\chi_m T$ reaches a value of 64.9 $cm^3$ K $mol^{-1}$ at 290 K which is slightly below the range 65.1–70.3 $cm^3$ K $mol^{-1}$ expected[27a] for five non-interacting $Dy^{3+}$ ($^6H_{15/2}$, $J = 15/2$, $g_J = 4/3$) centers. The decrease of $\chi_m T$ with lowering temperature is gradual down to ~100 K, and then more precipitous (approximate slope). This behavior and the low value of $\chi_m T$ at 290 K have their origin in the ligand field effect (*i.e.* depopulation of the $m_J$ sublevels) and potential antiferromagnetic exchange interactions within the compound (note that the distinct deviation from linear behavior in $\chi_m T$ is already introduced at higher temperatures $T \approx 200$ K). Analysis of the dc magnetic susceptibility data for **2** and **3** reveals similar behavior, and the $\chi_m T$ values at 290 K are also slightly lower than those expected for the respective number of non-interacting lanthanide centers. For **2**, $\chi_m T$ reaches 58.1 $cm^3$ K $mol^{-1}$ at 290 K (expected[27a] 58.2–60.1 $cm^3$ K $mol^{-1}$ for five non-interacting $Tb^{III}$ ($^7F_6$, $J = 6$, $g_J = 3/2$) centers); for **3**, $\chi_m T$ is 66.1 $cm^3$ K $mol^{-1}$

 

**Table 2** Structural and magnetic features of pentanuclear lanthanide assemblies

| Compound | Core topology | Coordination numbers (local geometries around Ln(III) centers) | Magnetic properties | Ref. |
|---|---|---|---|---|
| $[Dy_5(\mu_3\text{-}OH)_6(Acc)_6(H_2O)_{10}]\cdot Cl_9$ | Trigonal bipyramidal | Eight coordinated (distorted square-antiprism) | SMM<br>$U_{eff}$ = 1.91 K<br>$\tau_0 = 1.01 \times 10^{-6}$ s | 16*d* |
| Acc = 1-amino cyclohexane-1-carboxylic acid. | | | | |
| $[Dy_5O(O^iPr)_{13}]$<br>$^i$Pr = isopropyl | Square pyramidal | Six coordinated (octahedral) | SMM<br>$U_{eff}$ = 528 ± 11 K, 46.6 ± 0.7 K<br>$\tau_0 = 4.7 \times 10^{-10}$ s, $3.8 \times 10^{-6}$ s | 16*a* |
| $[Dy_5(OH)_5(\alpha\text{-}AA)_4(Ph_2acac)_6]$<br>α-AA = D-PhGly | Square pyramidal | Eight coordinated | SMM | 16*b* |
| $[Dy_5(\mu_3\text{-}OH)_3(opch)_6(H_2O)_3]$<br>$H_2$opch = *o*-vanillin pyrazine acylhydrazone | Butterfly | Eight coordinated (distorted dodecahedral), nine coordinated (distorted mono-capped square-antiprismatic) and nine coordinated (distorted triplecapped prismatic) | SMM<br>$U_{eff}$ = 8.1 ; 37.9 K<br>$\tau_0 = 1.7 \times 10^{-5}$ s; $9.7 \times 10^{-8}$ s | 16*e* |
| $[Dy_5(\mu_3\text{-}OH)_3(opch)_6(H_2O)_3](ClO_4)_2$<br>$H_2$opch = *o*-vanillin pyrazine acylhydrazone | Butterfly | Eight coordinated (distorted dodecahedral), nine coordinated (distorted mono-capped square-antiprismatic) and nine coordinated (distorted triplecapped prismatic) | SMM<br>$U_{eff}$ = 197 K ;<br>$\tau_0 = 3.2 \times 10^{-9}$ s | 16*e* |
| $[Dy_5(LH)_4(\eta^1\text{-}Piv)(\eta^2\text{-}Piv)_3\text{-}(\mu_2\text{-}\eta^2\ \eta^1 Piv)_2(H_2O)]\cdot Cl$ | [2.2] spirocycle | Eight coordinated (distorted triangulardodecahedral), eight coordinated (distorted square-antiprism) and nine coordinated (mono-capped-square-antiprism) | Slow relaxation | This work |




**Fig. 5** Temperature dependence of $\chi_m T$ of **1–3** at 0.1 Tesla; inset: molar magnetization $M_m$ as function of the applied field $B$ at 2 K.

at 290 K (expected[27a] 66.3–69.0 cm$^3$ K mol$^{-1}$ for five non-interacting $Ho^{III}$ ($^5I_8$, $J = 8$, $g_J = 5/4$) centers).

At 2 K, the molar magnetizations $M_m$ of **1–3** (Fig. 5, inset) indicate saturation and thus hint roughly at the ground state of the $Ln^{III}$ centers in each compound expected due to ligand field effects on the spin–orbit ground term, since the weak exchange interactions of lanthanides at zero field are eliminated by the applied maximum fields: all of the extrapolated saturation values are roughly right in the center between the minimum magnetization of the corresponding five non-interacting $Ln^{III}$ centers ($5g_J m_{J,min} N_A \mu_B$) and the maximum magnetization of such centers ($5g_J J N_A \mu_B$). This indicates that neither all $Ln^{III}$ centers of a compound are characterized by a ground state of minimal $m_{J,min}$ (±1/2 for **1**, 0 for **2**, **3**) nor by the maximum $m_J = J$.

A comprehensive model of compounds **1–3** based exclusively on the magnetic susceptibility data is not feasible because the description of the compounds should include at least two different lanthanide sites (approximately $D_{4d}$ and $D_{3h}$ symmetric, eight- or nine-fold coordinated centers) and three different exchange pathways. Without a simpler model system such as $\{Gd_5\}$, or complementary data such as from inelastic neutron scattering, degenerate preliminary solutions modeled by the computational framework CONDON 2.0[27b,c] cannot be ruled out. One feature common among all of these preliminary solutions provides qualitative insight into $\chi_m T$ and $M_m$ behavior presented in Fig. 5: all calculations reveal very weak ferromagnetic exchange interactions between the two outer lanthanides of each triangle (*i.e.* Ln1⋯Ln2 and Ln4⋯Ln5, Fig. 3b), and either antiferromagnetic (≈−0.3 cm$^{-1}$) or almost nonexistent exchange interactions for the remaining pathways (Ln1⋯Ln3, Ln2⋯Ln3, Ln3⋯Ln4, and Ln3⋯Ln5). Note that although the bridging ligands are similar, and thus exchange interactions might be assumed to be similar as well, the various distances between the Ln pairs and the presence of

three different site geometries, and thus ligand fields, explain the difference in the exchange interaction parameters.

Alternating current (ac) molar magnetic susceptibility measurements on complexes **1–3** revealed out-of-phase signals for the $Dy^{III}$ analogue **1**, but not for **2** and **3**, at zero dc field. The very small curvatures within the Argand plane for complex **1** (Fig. S3†) reveal in-phase signals $\chi'_m$ that are almost independent from the applied frequency (Fig. 6). The application of external static fields of up to 4000 G slightly shifted $\chi'_m$, but did not produce significantly greater curvatures for frequencies greater than 100 Hz. Similar behavior was observed by Thielemann *et al.*[16b] who ascribed it to a blocking temperature which lies significantly below the range explored by the magnetic measurements. Optimal slow relaxation magnetic measurements of complex **1** with respect to the experimental options at hand were obtained using a 3000 G static field, and a frequency range of 0.03 Hz–111 Hz (Fig. 7, insets Fig. 6). The in-phase ($\chi'_m$) and out-of-phase ($\chi''_m$) ac susceptibility components can be fitted to a Cole–Cole equation[28] for each temperature (Fig. 7, solid lines; Fig. S3†). To determine the average relaxation times of the magnetization under the optimized conditions, the temperature-dependent fit parameters have been analyzed using an Arrhenius expression ($\tau = \tau_0 \exp(\Delta U/k_B T)$). This results in an effective energy barrier $\Delta U = (5.2 \pm 0.5)$ cm$^{-1}$ and a time constant of $\tau_0 = (2.6 \pm 0.6) \times 10^{-2}$ s (Fig. S5†). In the generalized Debye model, the distribution width of $\tau$ is parameterized by the scalar $\alpha$. The nonzero mean value of $\alpha = 0.45 \pm 0.08$ reveals that several relaxation processes are active in this system. The time constant $\tau_0$ is anomalously large for SMM behavior, *i.e.* the entirely phenomenological parameter $\tau'_0$ does not fall within the typical SMM range, and indicates that rather a secondary relaxation process was observed in the presence of a bias field instead of the relaxation process indicated at zero field. This is supported by the occurrence of the minima in the Cole–Cole curves for higher frequencies (lower $\chi'_m$ values) hinting at further subsequent semi-circles which we could not enhance with the experimental set-up at hand. Since some or all exchange interactions within lanthanide compounds are overridden by the application of an external field of 3000 G, the observed process may be connected to a forced alignment of the momenta albeit further evidence is needed to prove this hypothesis.

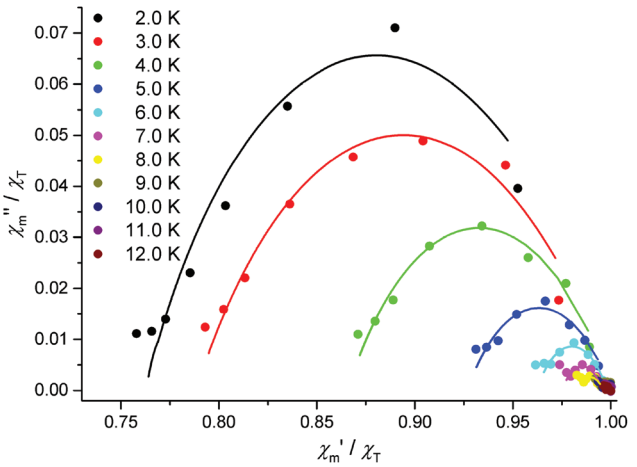


**Fig. 7** Normalized Cole–Cole plot of **1** at different temperatures and 3000 G dc field (solid circles), frequencies range from 0.03–111 Hz, $\chi_T$ is the isothermal susceptibility in the limit of lowest frequencies; fit to Cole–Cole equation (solid lines).

## Conclusions

In summary, a series of isostructural homometallic pentanuclear $Ln_5$ complexes that possess an unprecedented [2.2] spirocyclic topology were synthesized. The frameworks of these

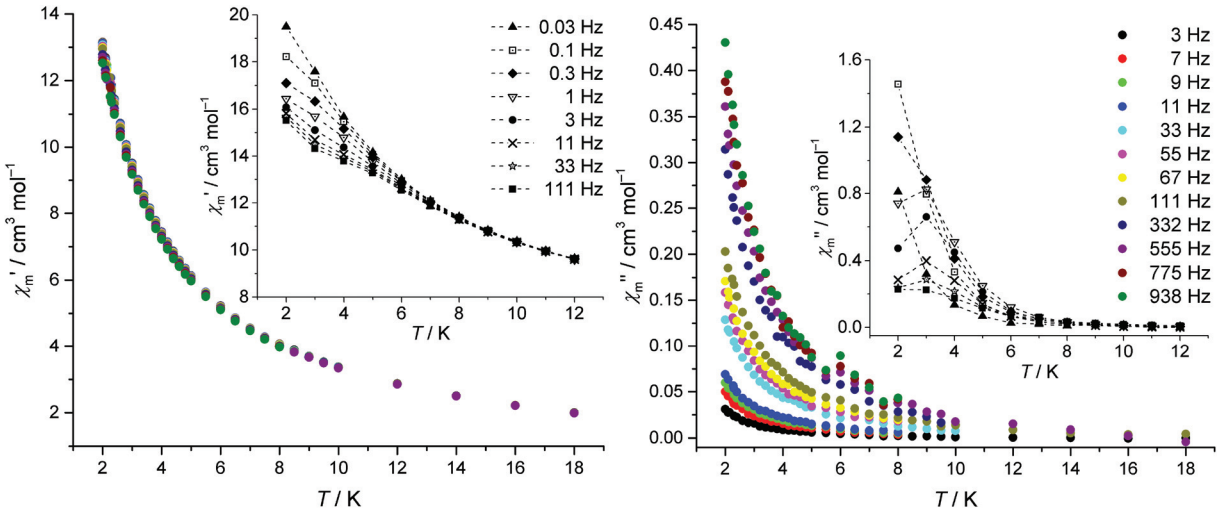


**Fig. 6** Left: in-phase magnetic susceptibility $\chi_m'$ *vs.* *T*; right: out-of-phase magnetic susceptibility $\chi_m''$ *vs.* *T* of **1** at different frequencies *f* at zero dc bias field; insets: at 3000 G dc bias field (dashed lines are guides for the eye).

 

complexes are comprised of the multidentate Schiff base ligand, *N*′-(2-hydroxy-3-(hydroxymethyl)-5-methylbenzylidene)-acetohydrazide, along with several bridging pivalate groups. The lanthanide centers present in the pentanuclear assembly can be grouped into three types based on their local coordination geometry: an eight-coordinate lanthanide in a distorted triangular dodecahedral geometry, an eight-coordinate lanthanide in a distorted square-antiprism geometry and a nine-coordinate lanthanide in a mono-capped square anti-prism geometry. Variable-temperature dc and ac magnetic susceptibility measurements reveal weak antiferromagnetic exchange interactions among the lanthanide centers of complexes **1–3**. Compound **1** exhibited temperature-dependent out-of-phase ac molar magnetic susceptibility signals with small curvatures at zero dc field. The application of a static 3000 G field intensified the ac magnetic susceptibility component, and an Arrhenius analysis confirmed the slow magnetic relaxation of the $Dy^{III}$ analogue.

# Experimental section

Solvents and other general reagents used in this work were purified according to the standard procedures.[29] 2,6-Bis(hydroxymethyl)-4-methylphenol, activated manganese(IV)dioxide ($MnO_2$), $DyCl_3{\cdot}6H_2O$, $TbCl_3{\cdot}6H_2O$ and $HoCl_3{\cdot}6H_2O$ were obtained from Sigma Aldrich Chemical Co. and were used as received. Acetyl hydrazide and 2-(hydroxymethyl)-6-carbaldehyde-4-methylphenol were prepared according to the literature procedure.[23e] Hydrazine hydrate (80%), pivalic acid and sodium sulphate (anhydrous) were obtained from S.D. Fine Chemicals, Mumbai, India and were used as such.

### Instrumentation

Melting points were measured using a JSGW melting point apparatus and are uncorrected. IR spectra were recorded as KBr pellets on a Bruker Vector 22 FT IR spectrophotometer operating at 400–4000 $cm^{-1}$. Elemental analyses of the compounds were obtained from Thermoquest CE instruments CHNS-O, EA/110 model. $^1H$ NMR spectra were recorded in $CD_3OD$ solutions on a JEOL JNM LAMBDA 400 model spectrometer operating at 500.0 MHz, chemical shifts are reported in parts per million (ppm) and are referenced with respect to internal tetramethylsilane ($^1H$). Powder X-ray diffraction (PXRD) patterns were recorded with a Bruker D8 advance diffractometer equipped with nickel-filtered Cu Kα radiation. Powder X-ray diffraction (PXRD) patterns of complexes **1–5** were in good agreement with the simulated patterns (ESI, Fig. S6–S8†). The difference in intensities could be due to the preferred orientation in the powder samples.

### Magnetic measurements

Magnetic susceptibility data of **1–3** were recorded using a Quantum Design MPMS-5XL SQUID magnetometer for static field (DC) and dynamic field (AC) measurements. The polycrystalline samples were compacted and immobilized into PTFE capsules. DC susceptibility data were acquired as a function of the field (0.1–5.0 T) and temperature (2–290 K). AC susceptibility data were measured at zero field and in the presence of various static fields in the frequency range 0.03–1000 Hz ($T$ = 1.8–50 K, $B_{ac}$ = 3 G, $B_{dc}$ = 0–4000 G). All data were corrected for the contribution of the sample holder (PTFE capsule) and the diamagnetic contributions of compounds **1–3** calculated from tabulated values ($-1.25 \times 10^{-3}$ $cm^3$ $mol^{-1}$, $-1.37 \times 10^{-3}$ $cm^3$ $mol^{-1}$ and $-1.32 \times 10^{-3}$ $cm^3$ $mol^{-1}$, respectively).

### X-ray crystallography

The crystal data for the compounds have been collected on a Bruker SMART CCD diffractometer (MoKα radiation, $\lambda$ = 0.71073 Å). The program SMART[30a] was used for collecting frames of data, indexing reflections, and determining lattice parameters, SAINT[30a] for integration of the intensity of reflections and scaling, SADABS[30b] for absorption correction, and SHELXTL[30c,d] for space group and structure determination and least-squares refinements on $F^2$. All the structures were solved by direct methods using the program SHELXS-97[30e] and refined by full-matrix least-squares methods against $F^2$ with SHELXL-97.[30e] Hydrogen atoms were fixed at calculated positions and their positions were refined by a riding model. All the non-hydrogen atoms were refined with anisotropic displacement parameters. The lattice solvent molecules of the complexes **1–3** cannot be modeled satisfactorily due to the presence of very high disorder. PLATON/SQUEEZE[30f,g] routine was utilized to remove the severely disordered solvent molecules. The total electron count thus squeezed is 396, 646 and 780 respectively per unit cell which corresponds to 99, 161 and 195 electrons per molecule ($Z$ = 4). These electron counts can be assigned to 5MeOH, $H_2O$ (expected 100) for **1**, $2CHCl_3$, 2MeOH, $H_2O$ (expected 162) for **2** and $2CHCl_3$, $8H_2O$ (expected 196) for **3**. The crystallographic figures have been generated using Diamond 3.1e software.[30h] The crystal data and the cell parameters for compounds **1–3** are summarized in Table 3. Crystallographic data (excluding structure factors) for the structures in this paper have been deposited with the Cambridge Crystallographic Data Centre as supplementary publication nos. CCDC 1031235–1031237.

### Synthesis

***N*′-(2-Hydroxy-3-(hydroxymethyl)-5-methylbenzylidene)acetohydrazide ($LH_3$).** To a stirred solution of 2-(hydroxymethyl)-6-carbaldehyde-4-methylphenol (1.50 g, 9.02 mmol) (**B2**) in 40 mL ethanol, acetyl hydrazide (0.66 g, 9.02 mmol) (**B1**) was added dropwise over a period of 15 minutes and the resultant yellow colored solution was refluxed for 5 h. Then, the yellow solution was concentrated *in vacuo* to 15 mL and kept in a refrigerator at 0 °C overnight. A light yellow colored heavy precipitate was obtained which was filtered and washed with cold ethanol as well as diethyl ether before being dried. Yield: 1.6 g (79.8%). Mp: 180 °C. FT-IR (KBr) $cm^{-1}$: 3398 $\nu$(O–H); 3181 $\nu$(N–H); 1661 $\nu$(C=O); 1624 $\nu(C{=}N)_{imine}$; 1516 $\nu$(C=N)py. $^1H$ NMR ($CD_3OD$, $\delta$, ppm, 500 MHz): 2.05 (s, 3H, $-CH_{3acetyl}$), 2.27 (s, 3H, $-CH_3$), 4.55 (s, 2H, $-CH_2OH$), 5.46 (s, 1H, $-OH_{phen}$), 7.02

Table 3 Crystal data and structure refinement parameters of **1–3**

| | 1 | 2 | 3 |
|---|---|---|---|
| Formula | $C_{148}H_{208}Cl_2Dy_{10}N_{16}O_{67}$ | $C_{148}H_{206}Cl_2N_{16}O_{69}Tb_{10}$ | $C_{148}H_{208}Cl_2Ho_{10}N_{16}O_{63}$ |
| $M$/g | 4979.22 | 4967.45 | 4939.52 |
| Crystal system | Tetragonal | Tetragonal | Tetragonal |
| Space group | $I\bar{4}$ | $I\bar{4}$ | $I\bar{4}$ |
| $a$/Å | 40.368(2) | 40.479(5) | 40.446(5) |
| $b$/Å | 40.368(2) | 40.479(5) | 40.446(5) |
| $c$/Å | 11.922(7) | 11.943(5) | 11.940(5) |
| $\alpha = \beta = \gamma$ (°) | 90 | 90 | 90 |
| $V$/Å$^3$ | 19 429(2) | 19 569(10) | 19 532(9) |
| $Z$ | 4 | 4 | 4 |
| $\rho_c$/g cm$^{-3}$ | 1.702 | 1.688 | 1.680 |
| $\mu$/mm$^{-1}$ | 3.905 | 3.674 | 4.107 |
| $F$(000) | 9752.0 | 9768.0 | 9664.0 |
| Cryst size (mm$^3$) | 0.09 × 0.078 × 0.023 | 0.12 × 0.07 × 0.06 | 0.15 × 0.11 × 0.06 |
| $\theta$ Range (°) | 2.26 to 26.80 | 2.25 to 28.04 | 2.25 to 20.39 |
| Limiting indices | $-43 \le h \le 51$ | $-51 \le h \le 50$ | $-49 \le h \le 29$ |
| | $-44 \le k \le 51$ | $-51 \le k \le 51$ | $-48 \le k \le 49$ |
| | $-15 \le l \le 14$ | $-15 \le l \le 12$ | $14 \le l \le 14$ |
| Reflns collected | 76 684 | 68 807 | 53 438 |
| Ind reflns | 21 174 [$R$(int) = 0.0722] | 21 266 [$R$(int) = 0.1230] | 18 181[$R$(int) = 0.0923] |
| Completeness to $\theta$ (%) | 99.9 | 99.8 | 100.0 |
| Refinement method | Full-matrix least-squares on $F^2$ | Full-matrix least-squares on $F^2$ | Full-matrix least-squares on $F^2$ |
| Data/restraints/params | 21 174/1/1068 | 21 266/22/1101 | 18 181/1/1081 |
| Goodness-of-fit on $F^2$ | 1.029 | 1.028 | 1.027 |
| Final $R$ indices [$I > 2\theta(I)$] | $R_1$ = 0.0501 | $R_1$ = 0.0565 | $R_1$ = 0.0676 |
| | w$R_2$ = 0.1065 | w$R_2$ = 0.1359 | w$R_2$ = 0.1536 |
| $R$ indices (all data) | $R_1$ = 0.0671 | $R_1$ = 0.0828 | $R_1$ = 0.1009 |
| | w$R_2$ = 0.1123 | w$R_2$ = 0.1532 | w$R_2$ = 0.1799 |

(s, 1H, Ar–H), 7.22 (s, 1H, Ar–H), 8.06 (s, 1H, –NH), 8.17 (s, 1H, imine). Anal. Calcd for $C_{11}H_{14}N_2O_3$: C, 59.45; H, 6.35; N, 12.60. Found: C, 58.77; H, 6.01; N, 12.19. ESI-MS, $m/z$: $(M + H)^+$. 223.09.

### General synthetic procedure for the preparation of complexes 1–3

All the pentanuclear complexes (**1–3**) have been synthesized according to the following procedure. $LH_3$ (0.04 g, 0.18 mmol) was dissolved in 40 mL methanol. To this solution, under stirring, $LnCl_3{\cdot}6H_2O$ (0.23 mmol) was added and the reaction mixture was stirred for 20 minutes at room temperature. At this stage, triethylamine (0.096 mL, 0.73 mmol) was added dropwise and the stirring was continued for a further 10 minutes and pivalic acid (0.028 g, 0.27 mmol) was added dropwise to the mixture. The resulting yellow colored solution was continuously stirred for 12 hours at room temperature. Then, the solution was completely evaporated *in vacuo* to afford a light yellow colored solid mass which was washed 2–3 times with diethyl ether and dried. The solid mass was re-dissolved in MeOH/$CHCl_3$ (1 : 1) and kept for crystallization. After about 12 days, needle-shaped yellow colored crystals suitable for X-ray crystallography were obtained by slow evaporation from the solvent mixture. Specific details of each reaction and the characterization data of the products obtained are given below.

**$[Dy_5(LH)_4(\eta^1\text{-Piv})(\eta^2\text{-Piv})_3(\mu_2\text{–}\eta^2\ \ \eta^1\text{Piv})_2(H_2O)]{\cdot}Cl{\cdot}9.5H_2O{\cdot}5$-MeOH (1).** Quantities: $LH_3$ (0.04 g, 0.18 mmol), $DyCl_3{\cdot}6H_2O$ (0.087 g, 0.23 mmol), $Et_3N$ (0.096 mL, 0.73 mmol), PivH (0.028 g, 0.27 mmol). Yield: 0.076 g, 63.3% (based on $Dy^{3+}$). Mp: 200 °C (d). IR (KBr) (cm$^{-1}$): 3433 (b), 2978 (s), 2950 (s), 2604 (s), 2497(s), 2343 (w), 1620 (s), 1574 (s), 1482 (s), 1429 (s), 1397 (s), 1309 (w), 1262 (w), 1228 (w), 1172 (w), 1072 (w), 1037 (s), 897 (w), 851 (w), 808 (s), 608 (w). Anal. Calcd for $C_{79}H_{122}Cl\ Dy_5\ N_8\ O_{39.5}$ (2663.80): C, 35.62; H, 4.62 N, 4.21. Found: C, 34.96; H, 4.33 N, 4.09.

**$[Tb_5(LH)_4(\eta^1\text{-Piv})(\eta^2\text{-Piv})_3(\mu_2\text{–}\eta^2\ \ \eta^1\text{Piv})_2(H_2O)]{\cdot}Cl{\cdot}10.5H_2O{\cdot}$ 2MeOH·2CHCl$_3$ (2).** Quantities: $LH_3$ (0.04 g, 0.18 mmol), $TbCl_3{\cdot}6H_2O$ (0.085 g, 0.23 mmol), $Et_3N$ (0.096 mL, 0.73 mmol), PivH (0.028 g, 0.27 mmol). Yield: 0.058 g, 46.03% (based on $Tb^{3+}$). Mp: 200 °C (d). IR (KBr) (cm$^{-1}$): 3441 (b), 2971 (s), 2930 (s), 2601 (s), 2499(s), 2339 (w), 1610 (s), 1570 (s), 1477(s), 1425 (s), 1393 (s), 1302 (w), 1252 (w), 1235 (w), 1178 (w), 1071 (w), 1032 (s), 895 (w), 854 (w), 803 (s), 610 (w). Anal. Calcd for $C_{78}H_{112}Cl_7N_8O_{37.5}Tb_5$ (2804.55): C, 33.40; H, 4.03; N, 4.00. Found: C, 32.93; H, 4.10 N, 4.04.

**$[Ho_5(LH)_4(\eta^1\text{-Piv})(\eta^2\text{-Piv})_3(\mu_2\text{–}\eta^2\eta^1\text{Piv})_2(H_2O)]{\cdot}Cl{\cdot}14.5$-$H_2O{\cdot}2CHCl_3$ (3).** Quantities: $LH_3$ (0.04 g, 0.18 mmol), $HoCl_3{\cdot}6H_2O$ (0.087 g, 0.23 mmol), $Et_3N$ (0.096 mL, 0.73 mmol), PivH (0.028 g, 0.27 mmol). Yield: 0.062 g, 48.4% (based on $Ho^{3+}$). Mp: 200 °C (d). IR (KBr) (cm$^{-1}$): 3447 (b), 2965 (s), 2933 (s), 2607 (s), 2497(s), 2331 (w), 1603 (s), 1579 (s), 1475(s), 1424 (s), 1390 (s), 1297 (w), 1251 (w), 1233 (w), 1172 (w), 1070 (w), 1029 (s), 899 (w), 844 (w), 798 (s), 611 (w). Anal. Calcd for $C_{76}H_{118}Cl_7Ho_5N_8O_{39.5}$ (2848.60): C, 32.04; H, 4.18; N, 3.93. Found: C, 31.73; H, 4.23; N, 3.61.

 

## Acknowledgements

We thank the Department of Science and Technology (DST), India, for financial support, including support for a Single Crystal CCD X-ray Diffractometer facility at IIT-Kanpur. V. C. is grateful to the DST for a J. C. Bose fellowship. S. B. thanks the Council of Scientific and Industrial Research, India for the Senior Research Fellowship.

## References

1 (*a*) P. W. Roesky, G. C. Melchor and A. Zulys, *Chem. Commun.*, 2004, 738; (*b*) P. W. Roesky and T. E. Muller, *Angew. Chem., Int. Ed.*, 2003, **42**, 2708; T. N. Parac-Vogt, K. Deleersnyder and K. Binnemans, *Eur. J. Org. Chem.*, 2005, 1810; (*c*) F. Pohlki and S. Doye, *Chem. Soc. Rev.*, 2003, **32**, 104; (*d*) X. Yu, S. Y. Seo and M. J. Tobin, *J. Am. Chem. Soc.*, 2007, **129**, 7244.

2 (*a*) M. Romanelli, G. A. Kumar, T. J. Emge, R. E. Riman and J. G. Brennan, *Angew. Chem., Int. Ed.*, 2008, **47**, 6049; (*b*) C. M. G. dos Santos, A. J. Harte, S. J. Quinn and T. Gunnlaugsson, *Coord. Chem. Rev.*, 2008, **252**, 2512; (*c*) S. L. Faulkner, S. Natrajan and D. Sykes, *Dalton Trans.*, 2009, 3890; (*d*) K. Binnemans, *Coord. Chem. Rev.*, 2009, **109**, 4283; (*e*) M. D. Ward, *Coord. Chem. Rev.*, 2007, **251**, 1663; (*f*) S. Sivakumar and M. L. P. Reddy, *J. Mater. Chem.*, 2012, **22**, 10852.

3 (*a*) A. Picot, A. D'Alé, P. L. Baldeck, A. Grichine, A. Duperray, C. Andraud and O. Maury, *J. Am. Chem. Soc.*, 2008, **130**, 1532; (*b*) M. Bottrill, L. Kwok and N. Long, *J. Chem. Soc. Rev.*, 2006, **35**, 557.

4 (*a*) S. Biswas, H. S. Jena, A. Adhikary and S. Konar, *Inorg. Chem.*, 2014, **53**, 3926; (*b*) S. Goswami, A. Adhikary, H. S. Jena and S. Konar, *Dalton Trans.*, 2013, **42**, 9813; (*c*) J. A. Sheikh, A. Adhikary and S. Konar, *New J. Chem.*, 2014, **38**, 3006; (*d*) L. Bogani and W. Wernsdorfer, *Nat. Mater.*, 2008, **7**, 179; (*e*) Y.-Z. Zheng, M. Evangelisti and R. E. P. Winpenny, *Angew. Chem., Int. Ed.*, 2011, **50**, 3692; (*f*) Y.-Z. Zheng, M. Evangelisti, F. Tuna and R. E. P. Winpenny, *J. Am. Chem. Soc.*, 2012, **134**, 1057; (*g*) Y.-Z. Zheng, M. Evangelisti and R. E. P. Winpenny, *Chem. Sci.*, 2011, **2**, 99; (*h*) J. M. Jia, S. J. Liu, Y. Cui, S. D. Han, T.-L. Hu and X. H. Bu, *Cryst. Growth Des.*, 2013, **13**, 4631.

5 (*a*) M. Affronte, *J. Mater. Chem.*, 2009, **19**, 1731; (*b*) A. R. Rocha, V. García-Suárez, S. W. Bailey, C. J. Lambert, J. Ferrerand and S. Sanvito, *Nat. Mater.*, 2005, **4**, 335; (*c*) M. Urdampilleta, S. Klyatskaya, J.-P. Cleuziou, M. Ruben and W. Wernsdorfer, *Nat. Mater.*, 2011, **10**, 502.

6 (*a*) J. D. Rinehart, M. Fang, W. J. Evans and J. R. Long, *J. Am. Chem. Soc.*, 2011, **133**, 14236; (*b*) J. D. Rinehart, M. Fang, W. J. Evans and J. R. Long, *Nat. Chem.*, 2011, **3**, 538; (*c*) M. Urdampilleta, S. Klyatskaya, J. P. Cleuziou, M. Ruben and W. Wernsdorfer, *Nat. Mater.*, 2011, **10**, 502; (*d*) L. Bogani and W. Wernsdorfer, *Nat. Mater.*, 2008, **7**, 179.

7 (*a*) A. Ardavan and S. J. Blundell, *J. Mater. Chem.*, 2009, **19**, 1754; (*b*) F. Troiani and M. Affronte, *Chem. Soc. Rev.*, 2011, **40**, 3119; (*c*) P. C. E. Stamp and A. Gaita-Ariño, *J. Mater. Chem.*, 2009, **19**, 1718; (*d*) J. Lehmann, A. Gaita-Ariño, E. Coronado and D. Loss, *Nat. Nanotechnol.*, 2007, **2**, 312; (*e*) M. N. Leuenberger and D. Loss, *Nature*, 2001, **410**, 789.

8 (*a*) R. Sessoli, L. Hui, A. R. Schake, S. Wang, J. B. Vincent, K. Folting, D. Gatteschi and G. Christou, *J. Am. Chem. Soc.*, 1993, **115**, 1804; (*b*) R. Sessoli, D. Gatteschi, A. Caneschi and M. A. Novak, *Nature*, 1993, **365**, 141; (*c*) J.-P. Zhao, B. W. Hu, X. F. Zhang, Q. Yang, M. S. El Fallah, J. Ribas and X. H. Bu, *Inorg. Chem.*, 2010, **49**, 11325.

9 (*a*) D. W. Boukhvalov, V. V. Dobrovitski, P. Kögerler, M. Al-Saqer, M. I. Katsnelson, A. I. Lichtenstein and B. N. Harmon, *Inorg. Chem.*, 2010, **49**, 10902; (*b*) T. Glaser, *Chem. Commun.*, 2011, **47**, 116; (*c*) A. Grigoropoulos, M. Pissas, P. Papatolis, V. Psycharis, P. Kyritsis and Y. Sanakis, *Inorg. Chem.*, 2013, **52**, 12869; (*d*) A. K. Boudalis, M. Pissas, C. P. Raptopoulou, V. Psycharis, B. Abarca and R. Ballesteros, *Inorg. Chem.*, 2008, **47**, 10674; (*e*) G. Lazari, T. C. Stamatatos, C. P. Raptopoulou, V. Psycharis, M. Pissas, S. P. Perlepes and A. K. Boudalis, *Dalton Trans.*, 2009, 3215; (*f*) M. Shanmugam, S. Vaidya, A. Upadhyay, S. K. Singh, T. Gupta, S. Tewary, S. Langley, J. Walsh, K. S. Murray and G. Rajaraman, *Chem. Commun.*, 2015, **51**, 3739–3742.

10 (*a*) S. Osa, T. Kido, N. Matsumoto, N. Re, A. Pochaba and J. Mrozinski, *J. Am. Chem. Soc.*, 2004, **126**, 420; (*b*) C. M. Zaleski, E. C. Depperman, J. W. Kampf, M. L. Kirk and V. L. Pecoraro, *Angew. Chem., Int. Ed.*, 2004, **43**, 3912; (*c*) T. K. Prasad, M. V. Rajasekharan and J. P. Costes, *Angew. Chem., Int. Ed.*, 2007, **46**, 2851; (*d*) G. P. Guedes, S. Soriano, L. A. Mercante, N. L. Speziali, M. A. Novak, M. Andruh and M. G. F. Vaz, *Inorg. Chem.*, 2013, **52**, 8309; (*e*) J. Ruiz, G. Lorusso, M. Evangelisti, E. K. Brechin, S. J. A. Pope and E. Colacio, *Inorg. Chem.*, 2014, **53**, 3586; (*f*) M. A. Palacios, S. T.-Padilla, J. Ruiz, J. M. Herrera, S. J. A. Pope, E. K. Brechin and E. Colacio, *Inorg. Chem.*, 2014, **53**, 1465; (*g*) A. Upadhyay, S. K. Singh, C. Das, R. Mondol, S. K. Langley, K. S. Murray, G. Rajaraman and M. Shanmugam, *Chem. Commun.*, 2014, **50**, 8838; (*h*) Y. F. Zeng, G. C. Xu, X. Hu, Z. Chen, X. H. Bu, S. Gao and E. C. Sañudo, *Inorg. Chem.*, 2010, **49**, 9734; (*i*) S.-D. Han, S.-J. Liu, Q.-L. Wang, X.-H. Miao, T.-L. Hu and X.-H. Bu, *Cryst. Growth Des.*, 2015, **15**, 2253; (*j*) S.-J. Liu, Y.-F. Zeng, L. Xue, S.-D. Han, J.-M. Jia, T.-L. Hu and X. H. Bu, *Inorg. Chem. Front.*, 2014, **1**, 200.

11 (*a*) R. J. Blagg, L. Ungur, F. Tuna, J. Speak, P. Comar, D. Collison, W. Wernsdorfer, E. J. L. McInnes, L. F. Chibotaru and R. E. P. Winpenny, *Nat. Chem.*, 2013, **5**, 673; (*b*) R. J. Blagg, C. A. Muryn, E. J. L. McInnes, F. Tuna and R. E. P. Winpenny, *Angew. Chem., Int. Ed.*, 2011, **50**, 6530.

12 (*a*) E. Lucaccini, L. Sorace, M. Perfetti, J.-P. Costes and R. Sessoli, *Chem. Commun.*, 2014, **50**, 1648; (*b*) F. Gao, L. Cui, Y. Song, Y.-Z. Li and J.-L. Zuo, *Inorg. Chem.*, 2014,

**53**, 562; (*c*) J. J. Baldoví, S. C. Serra, J. M. Clemente-Juan, E. Coronado, A. G. Arin and A. Palii, *Inorg. Chem.*, 2012, **51**, 12565; (*d*) G. Rajaraman, S. K. Singh, T. Gupta and M. Shanmugam, *Chem. Commun.*, 2014, **50**, 15513–15516.

13 (*a*) P.-H. Lin, T. J. Burchell, R. Clerac and M. Murugesu, *Angew. Chem., Int. Ed.*, 2008, **47**, 8848; (*b*) G.-F. Xu, Q.-L. Wang, P. Gamez, Y. Ma, R. Cl_erac, J. Tang, S.-P. Yan, P. Cheng and D.-Z. Liao, *Chem. Commun.*, 2010, **46**, 1506; (*c*) K. A. Thiakou, V. Bekiari, C. P. Raptopoulou, V. Psycharis, P. Lianos and S. P. Perlepes, *Polyhedron*, 2006, **25**, 2869; (*d*) S.-S. Bao, L.-F. Ma, Y. Wang, L. Fang, C.-J. Zhu, Y.-Z. Li and L.-M. Zheng, *Chem. – Eur. J.*, 2007, **13**, 2333; (*e*) S. J. Liu, J.-P. Zhao, W.-C. Song, S.-D. Han, Z.-Y. Liu and X.-H. Bu, *Inorg. Chem.*, 2013, **52**, 2103.

14 (*a*) I. J. Hewitt, Y. Lan, C. E. Anson, J. Luzon, R. Sessoli and A. K. Powell, *Chem. Commun.*, 2009, 6765; (*b*) J. Tang, I. J. Hewitt, T. N. Madhu, G. Chastanet, W. Wernsdorfer, C. E. Anson and A. K. Powell, *Angew. Chem., Int. Ed.*, 2006, **45**, 1729; (*c*) M. U. Anwar, S. S. Tandon, L. N. Dawe, F. Habib, M. Murugesu and L. K. Thompson, *Inorg. Chem.*, 2012, **51**, 1028.

15 (*a*) B.-Q. Ma, D.-S. Zhang, S. Gao, T.-Z. Jin, C.-H. Yan and G.-X. Xu, *Angew. Chem., Int. Ed.*, 2000, **39**, 3644; (*b*) Y. Gao, G.-F. Xu, Z. L. Hao, J. Tang and Z. Liu, *Inorg. Chem.*, 2009, **48**, 11495; (*c*) Y. Bi, X.-T. Wang, W. Liao, X. Wang, R. Deng, H. Zhang and S. Gao, *Inorg. Chem.*, 2009, **48**, 11743; (*d*) N. M. Randell, M. U. Anwar, M. W. Drover, L. N. Dawe and L. K. Thompson, *Inorg. Chem.*, 2013, **52**, 6731; (*e*) S.-D. Han, X.-H. Miao, S.-J. Liu and X.-H. Bu, *Inorg. Chem. Front.*, 2014, **1**, 549; (*f*) F. C. Liu, Y.-F. Zeng, J.-P. Zhao, B. W. Hu, X. Hu, J. Ribasc and X. H. Bu, *Dalton Trans.*, 2009, 2074.

16 (*a*) R. J. Blagg, C. A. Muryn, E. J. L. McInnes, F. Tuna and R. E. P. Winpenny, *Angew. Chem., Int. Ed.*, 2011, **50**, 6530; (*b*) D. T. Thielemann, A. T. Wagner, Y. Lan, C. E. Anson, M. T. Gamer, A. K. Powell and P. W. Roesky, *Dalton Trans.*, 2013, **42**, 14794; (*c*) M. T. Gamer, Y. Lan, P. W. Roesky, A. K. Powell and R. Clérac, *Inorg. Chem.*, 2008, **47**, 6581; (*d*) J.-B. Peng, X.-J. Kong, Y.-P. Ren, L.-S. Long, R.-B. Huang and L.-S. Zheng, *Inorg. Chem.*, 2012, **51**, 2186; (*e*) H. Tian, L. Zhao, H. Lin, J. Tang and G. Li, *Chem. – Eur. J.*, 2013, **19**, 13235.

17 (*a*) D.-S. Zhang, B.-Q. Ma, T.-Z. Jin, S. Gao, C.-H. Yan and T. C. W. Mak, *New J. Chem.*, 2000, **24**, 61; (*b*) N. Mahe, O. Guillou, C. Daiguebonne, Y. G_erault, A. Caneschi, C. Sangregorio, C. J. Y. Hane-Ching, P. E. Car and T. Roisnel, *Inorg. Chem.*, 2005, **44**, 7743; (*c*) B. Hussain, D. Savard, T. J. Burchell, W. Wernsdorfer and M. Murugesu, *Chem. Commun.*, 2009, 1100; (*d*) S. Xue, L. Zhao, Y. N. Guo, P. Zhang and J. K. Tang, *Chem. Commun.*, 2012, **48**, 8946; (*e*) L. Ungur, S. K. Langley, T. N. Hooper, B. Moubaraki, E. K. Brechin, K. S. Murray and L. F. Chibotaru, *J. Am. Chem. Soc.*, 2012, **134**, 18554.

18 X.-J. Zheng, L.-P. Jin and S. Gao, *Inorg. Chem.*, 2004, **43**, 1600.

19 (*a*) T. Kajiwara, H. Wu, T. Ito, N. Iki and S. Miyano, *Angew. Chem., Int. Ed.*, 2004, **43**, 1832; (*b*) V. Chandrasekhar, P. Bag and E. Colacio, *Inorg. Chem.*, 2013, **52**, 4562–4570.

20 (*a*) G. Xu, Z.-M. Wang, Z. He, Z. Lü, C.-S. Liao and C.-H. Yan, *Inorg. Chem.*, 2002, **41**, 6802; (*b*) G.-F. Xu, P. Gamez, S. J. Teat and J. Tang, *Dalton Trans.*, 2010, **39**, 4353.

21 (*a*) K. Manseki and S. Yanagida, *Chem. Commun.*, 2007, 1242; (*b*) L. G. Westin, M. Kritikos and A. Caneschi, *Chem. Commun.*, 2003, 1012; (*c*) X. Yang, R. A. Jones and M. J. Wiester, *Dalton Trans.*, 2004, 1787; (*d*) A. Kornienko, T. J. Emge, G. A. Kumar, R. E. Riman and J. G. Brennan, *J. Am. Chem. Soc.*, 2005, **127**, 3501.

22 (*a*) P. C. Andrews, T. Beck, C. M. Forsyth, B. H. Fraser, P. C. Junk, M. Massi and P. W. Roesky, *Dalton Trans.*, 2007, 5651; (*b*) R. Wang, H. D. Selby, H. Liu, M. D. Carducci, T. Jin, Z. Zheng, J. W. Anthis and R. J. Staples, *Inorg. Chem.*, 2002, **41**, 278.

23 (*a*) V. Chandrasekhar, B. M. Pandian, R. Azhakar, J. J. Vittal and R. Clérac, *Inorg. Chem.*, 2007, **46**, 5140; (*b*) V. Chandrasekhar, B. M. Pandian, R. Boomishankar, A. Steiner, J. J. Vittal, A. Houri and R. Clérac, *Inorg. Chem.*, 2008, **47**, 4918; (*c*) V. Chandrasekhar, P. Bag, W. Kroener, K. Gieb and P. Müller, *Inorg. Chem.*, 2013, **52**, 13078; (*d*) V. Chandrasekhar, S. Das, A. Dey, S. Hossain, F. Lloret and E. Pardo, *Eur. J. Inorg. Chem.*, 2013, 4506; (*e*) V. Chandrasekhar, S. Das, A. Dey, S. Hossain, S. Kundu and E. Colacio, *Eur. J. Inorg. Chem.*, 2014, 397; (*f*) C. Meseguer, S. T.-Padilla, M. M. Hänninen, R. Navarrete, A. J. Mota, M. Evangelisti, J. Ruiz and E. Colacio, *Inorg. Chem.*, 2014, **53**, 12092–12099; (*g*) A. Deb, T. T. Boron, M. Itou, Y. Sakurai, T. Mallah, V. L. Pecoraro and J. E. Penner-Hahn, *J. Am. Chem. Soc.*, 2014, **136**, 4889; (*h*) C. M. Zaleski, J. W. Kampf, T. Mallah, M. L. Kirk and V. L. Pecoraro, *Inorg. Chem.*, 2007, **46**, 1954; (*i*) J. Goura, R. Guillaume, E. Rivière and V. Chandrasekhar, *Inorg. Chem.*, 2014, **53**, 7815; (*j*) P. Bag, A. Chakraborty, G. Rogez and V. Chandrasekhar, *Inorg. Chem.*, 2014, **53**, 6524.

24 (*a*) S. Das, S. Hossain, A. Dey, S. Biswas, J.-P. Sutter and V. Chandrasekhar, *Inorg. Chem.*, 2014, **53**, 5020–5028; (*b*) V. Chandrasekhar, P. Bag and E. Colacio, *Inorg. Chem.*, 2013, **52**, 4562; (*c*) S. Das, S. Hossain, A. Dey, S. Biswas, J.-P. Sutter and V. Chandrasekhar, *Inorg. Chem.*, 2014, **53**, 5020–5028; (*d*) T. Fukuda, N. Shigeyoshi, T. Yamamura and N. Ishikawa, *Inorg. Chem.*, 2014, **53**, 9080; (*e*) J. J. Le Roy, L. Ungur, I. Korobkov, L. F. Chibotaru and M. Murugesu, *J. Am. Chem. Soc.*, 2014, **136**, 8003; (*f*) F. Habib, G. Brunet, V. Vieru, I. Korobkov, L. F. Chibotaru and M. Murugesu, *J. Am. Chem. Soc.*, 2013, **135**, 13242; (*g*) V. E. Campbell, H. Bolvin, E. Rivière, R. Guillot, W. Wernsdorfer and T. Mallah, *Inorg. Chem.*, 2014, **53**, 2598.

25 V. Chandrasekhar, S. Hossain, S. Das, S. Biswas and J.-P. Sutter, *Inorg. Chem.*, 2013, **52**, 6346.

26 S. Das, A. Dey, S. Biswas, E. Colacio and V. Chandrasekhar, *Inorg. Chem.*, 2014, **53**, 3417.

27 (*a*) H. Lueken, *Magnetochemie*, Teubner, Stuttgart, Germany, 1999; (*b*) M. Speldrich, H. Schilder, H. Lueken

 

and P. Kögerler, *Isr. J. Chem.*, 2011, **51**, 215–227; (*c*) J. van Leusen, M. Speldrich, H. Schilder and P. Kögerler, *Coord. Chem. Rev.*, 2015, **289–290**, 137–148.

28 K. S. Cole and R. H. Cole, *J. Chem. Phys.*, 1941, **9**, 341–351.

29 (*a*) *Vogel's Textbook of Practical Organic Chemistry*, ed. B. S. Furniss, A. J. Hannaford, P. W. G. Smith and A. R. Tatchell, ELBS and Longman, London, 5th edn, 1989; (*b*) D. B. G. Williams and M. Lawton, *J. Org. Chem.*, 2010, **75**, 8351–8354; (*c*) X. Zeng, D. Coquiére, A. Alenda, E. Garrier, T. Prangé, Y. Li, O. Reinaud and I. Jabin, *Chem. – Eur. J.*, 2006, **12**, 6393–6402.

30 (*a*) *SMART & SAINT Software Reference manuals, Version 6.45*, Bruker Analytical X-ray Systems, Inc., Madison, WI, 2003; (*b*) G. M. Sheldrick, *SADABS, a software for empirical absorption correction, Ver. 2.05*, University of Göttingen, Göttingen, Germany, 2002; (*c*) *SHELXTL Reference Manual, Ver. 6.1*, Bruker Analytical X-ray Systems, Inc., Madison, WI, 2000; (*d*) G. M. Sheldrick, *SHELXTL, Ver. 6.12*, Bruker AXS Inc., Madison, WI, 2001; (*e*) G. M. Sheldrick, *SHELXL97, Program for Crystal Structure Refinement*, University of Göttingen, Göttingen, Germany, 1997; (*f*) P. Van der Sluis and A. L. Spek, *Acta Crystallogr., Sect. A: Found. Crystallogr.*, 1990, **46**, 194; (*g*) A. L. Spek, *Acta Crystallogr., Sect. A: Found. Crystallogr.*, 1990, **46**, c34; (*h*) K. Bradenburg, *Diamond, Ver. 3.1eM*, Crystal Impact GbR, Bonn, Germany, 2005.